Applied Meteorology Unit (AMU)

Quarterly Report

First Quarter FY-01

Contract NAS10-96018

31 January 2001

ENSCO, Inc.
1980 N. Atlantic Ave., Suite 230
Cocoa Beach, FL 32931
(321) 853-8202 (AMU)
(321) 783-9735

Distribution:

NASA HQ/Q/F. Gregory
NASA KSC/AA/R. Bridges
NASA KSC/MK/J. Halsell
NASA KSC/PH/D. King
NASA KSC/PH/E. Mango
NASA KSC/PH/M. Leinbach
NASA KSC/PH/M. Wetmore
NASA KSC/PH-A/J. Guidi
NASA KSC/YA/K. Payne
NASA KSC/YA-C/D. Bartine
NASA KSC/YA-D/H. Delgado
NASA KSC/YA-D/J. Madura
NASA KSC/YA-D/F. Merceret
NASA KSC/YA-C/G. Allen
NASA JSC/DA8/W. Hale
NASA JSC/MA/R. Dittemore
NASA JSC/MS4/J. Richart
NASA JSC/MS4/R. Adams
NASA JSC/ZS8/F. Brody
NASA MSFC/ED03/S. Pearson
NASA MSFC/ED44/D. Johnson
NASA MSFC/ED44/B. Roberts
NASA MSFC/ED44/G. Jasper
NASA MSFC/MP01/A. McCool
NASA MSFC/MP71/S. Glover
45 WS/CC/N. Wyse
45 WS/DO/M. Christie
45 WS/DOR/D. Beberwyk
45 WS/DOR/D. McCabe
45 WS/DOR/J. Sardonia
45 WS/DOR/J. Tumbiolo
45 WS/DOR/E. Priselac
45 WS/DOR/J. Weems
45 WS/SY/D. Harms
45 WS/SYR/W. Roeder
45 WS/SYA/B. Boyd
45 OG/CC/D. Mitchell
45 LG/CC/S. Fancher
45 LG/LGP/R. Fore
CSR 7000/M. Maier
CSR 4140/H. Herring
45 SW/SESL/D. Berlinrut
SMC/CWP/M. Coolidge
SMC/CWP/T. Knox
SMC/CWP/R. Bailey
SMC/CWP (PRC)/P. Conant
Hq AFSPC/DORW/S. Carr
Hq AFWA/CC/C. French
Hq AFWA/DNX/E. Bensman
Hq AFWA/DN/N. Feldman
Hq USAF/XOW/H. Tileston
Hq AFRL/XPPR/B. Bauman

Office of the Federal Coordinator for Meteorological Services and Supporting Research
SMC/SDEW/L. Hagerman
NOAA “W/NP”/L. Uccellini
NOAA/OAR/SSMC-I/J. Golden
NOAA/ARL/J. McQueen
NOAA Office of Military Affairs/L. Freeman
Aerospace Corp/T. Adang
NWS Melbourne/B. Hagemeyer
NWS Southern Region HQ/“W/SRH”/X. W. Proenza
NWS Southern Region HQ/“W/SR3”/D. Smith
NSSL/D. Forsyth
NWS/“W/OSD5”/B. Saffle
FSU Department of Meteorology/P. Ray
NCAR/J. Wilson
NCAR/Y. H. Kuo
30 WS/SY/C. Crosiar
30 WS/CC/P. Boerlage
30 SW/XP/J. Hetrick
NOAA/ERL/FSL/J. McGinley
ENSCO Contracts/E. Lambert

Executive Summary

This report summarizes the Applied Meteorology Unit (AMU) activities for the first quarter of Fiscal Year 01 (October – December 2000). A detailed project schedule is included in the Appendix.

Ms. Lambert continued work on the Statistical Short-Range Forecast Tools task with the goal of developing short-range ceiling forecast equations to be used in support of Shuttle landings. Using 19 years of cool-season (October – March) data, she developed and tested 1- and 2-hour observations-based and persistence climatology forecast equations that predict ceiling probabilities at the Shuttle Landing Facility. The observations-based forecasts showed a definite improvement over the persistence climatology forecasts. Based on these results, Ms. Lambert will develop and test 3-hour forecast equations.

Dr. Short continued Phase II of the IRIS SIGMET Processor Evaluation task. He is developing products to meet the operational requirements of the 45th Weather Squadron (45 WS) and the Spaceflight Meteorology Group (SMG) using SIGMET Inc.'s Interactive Radar Information System (IRIS) on the Weather Surveillance Radar, Model 74C (WSR-74C) located at Patrick Air Force Base. To aid in the development of seasonal scan strategies, Dr. Short developed a generalized method for determining the sequence of radar elevation angles that comprise a radar scan strategy. The method will compare the vertical resolutions of alternative scan strategies and enable an evaluation of the impact of scan strategy changes on vertical resolution. This will be important in determining the appropriate scan strategy for each season of the year.

Mr. Wheeler and Mr. Dianic began preparations for the Airborne Field Mill (ABFM) campaign scheduled for February 2001. The ABFM experiment will collect data to allow safe revision of the lightning launch commit criteria to provide greater launch availability. The AMU was tasked to superimpose the location of the ABFM research aircraft on WSR-74C radar images for the June 2000 campaign. During the June campaign, several issues with the display were noted and will be addressed by Mr. Wheeler and Mr. Dianic prior to the February 2001 campaign.

Mr. Wheeler and Dr. Short began work on the Mini-SODAR evaluation. The mini-SODAR is an acoustic wind profiler that provides a high spatial and temporal resolution vertical profile of wind speed and direction. Boeing plans to install a mini-SODAR at the new Space Launch Complex 37 as a substitute for a tall wind tower to evaluate the launch pad winds during ground and launch operations. In order to make critical GO/NO GO launch decisions, forecasters need to know the quality of the mini-SODAR data. Therefore, Mr. Wheeler and Dr. Short will perform an objective comparison between the SLC-37 mini-SODAR wind observations and those from the closest tall (≥ 204 ft) wind towers.

Mr. Case continued the evaluation of the Regional Atmospheric Modeling System (RAMS) component of the Eastern Range Dispersion Assessment System (ERDAS). Mr. Case completed most components of the objective and subjective evaluations of RAMS. For the objective evaluation, he compiled point error statistics for both the 1999-2000 cool (November to March) and 2000 warm seasons (May to September), and generated point error statistics under various meteorological regimes for the 2000 warm-season. For the subjective evaluation, Mr. Case completed the sea-breeze verification for the 1999 and 2000 warm-seasons. He also compiled error statistics for a subjective precipitation and thunderstorm initiation verification.

Mr. Case continued work on Phase III of the Local Data Integration System (LDIS) task, which calls for AMU assistance to install a working LDIS at SMG and the National Weather Service in Melbourne (NWS MLB) that generates routine high-resolution products for operational guidance. He helped SMG to correct a problem in the cloud analysis portion of the LDIS, and worked with NWS MLB toward solving their data ingest problems.

Mr. Dianic continued work on the Extension/Enhancement of the ERDAS RAMS Evaluation task to improve the archived database, and to perform sensitivity tests to identify the possible cause(s) of the model cold bias. He conducted a RAMS simulation using the Eta 0-hour forecasts as the background field, and ran a sensitivity experiment using an alternative radiation scheme in place of the current scheme. In addition, Mr. Dianic installed and tested ERDAS RAMS on an AMU workstation, and continued to develop a possible real-time data transfer mechanism that will be able to send RAMS forecast output to SMG and NWS MLB.

Table of Contents

SPECIAL NOTICE TO READERS

AMU Quarterly Reports are temporarily unavailable on the Wide World Web (WWW). Notice of its availability will be posted in this section.

The AMU Quarterly Reports are also available in electronic format via email. If anyone on the current distribution would like to be added to the email list, please send your email address to Winifred Lambert (321-853-8130, lambert.winifred@ensco.com). If any of your mailing information changes or if you would like to be removed from the distribution list, please notify Frank Merceret (321-867-0818, francis.merceret-1@ksc.nasa.gov) or Winifred Lambert (321-853-8130, lambert.winifred@ensco.com).

1. BACKGROUND

The AMU has been in operation since September 1991. Tasking is determined annually with reviews at least semi-annually. The progress being made in each task is discussed in Section 2 with the primary AMU point of contact reflected on each task and/or subtask. A list of acronyms used in this report immediately follows Section 2.

2. AMU ACCOMPLISHMENTS DURING THE PAST QUARTER

2.1 TASK 003 SHORT-TERM FORECAST IMPROVEMENT

SUBTASK 3 STATISTICAL SHORT-RANGE FORECAST TOOLS (MS. LAMBERT)

The forecast cloud ceiling at the Shuttle Landing Facility (SLF) is a critical element in determining whether a GO or NO GO should be issued for a Space Shuttle landing. However, the Spaceflight Meteorology Group (SMG) forecasters have found that ceiling is a difficult parameter to forecast. The goal of this task is to develop short-range ceiling forecast equations to be used in support of Shuttle landings. Ms. Lambert is using a 19-year record (1979–1997) of hourly surface observations from the SLF and several stations in east-central Florida to develop these equations. The equation development is centered on the ceiling thresholds defined by the Shuttle Flight Rules (FRs) and shown in Table 1.

Table 1. List of Flight Rules for ceiling thresholds at the Shuttle Landing Facility (SLF).

Ceiling Threshold	***Flight Rule***
< 5000 ft	Return to Launch Site (RTLS)
< 8000 ft	End of Mission (EOM)
< 10 000 ft	Navigation Aid Degradation

During this quarter, Ms. Lambert developed forecast equations for the SLF following the procedures outlined in Vislocky and Fritsch (1997) and Hilliker and Fritsch (1999). Both studies showed that observations-based forecast equations, developed with data from the station of interest and its surrounding stations, performed better in the short-term (< 6 hours) than persistence climatology. Vislocky and Fritsch (hereafter VF) contended that persistence climatology is a strong benchmark against which to test the skill of any short-term forecast model. This confirmed the improved skill of their observations-based forecasts. For this task, surface observation data from the SLF (TTS, 3-letter identifier) and other central Florida stations were used to develop observations-based (OBS) equations. Data from TTS only was used to develop the persistence climatology (PCLIMO) equations according to VF.

Ms. Lambert used a 16-year subset of the data (*i.e.* dependent data) to create both the OBS and PCLIMO equations. Equations for 1- and 2-hour forecasts were created for each ceiling category (3) and for each hour of the day (24) during the cool season (October – March), resulting in 144 equations each for the OBS and PCLIMO methods. The equations were tested using the remaining 3-year subset of the data (*i.e.* independent data). Both the OBS and PCLIMO equations produce probability forecasts with values between 0 and 1. The value indicates the probability of occurrence of a particular ceiling category at a certain time.

The Brier scores (B) for both methods were calculated using the equation

$$\mathrm{B} = \frac{1}{n}\sum_{i=1}^{n}(f_i - o_i)^2,$$

where n is the number of forecast/observation pairs, f is the probability forecast value, and o is the observation value (0 or 1). B is 0 for perfect forecasts and 1 for completely incorrect forecasts. The Brier scores for the OBS and PCLIMO predictions were then used in the following equation

$$\mathrm{S} = \frac{(\mathrm{B}_{obs} - \mathrm{B}_{pclimo})}{(\mathrm{B}_{perfect} - \mathrm{B}_{pclimo})} \times 100,$$

where S is the Skill score, B_{obs} is the OBS Brier score, B_{pclimo} is the PCLIMO Brier score, and $\mathrm{B}_{perfect}$ is a perfect Brier score, which is 0. If the Skill score is positive, it indicates a percent improvement of the OBS method over the PCLIMO method. A negative value would indicate that the PCLIMO method produces a more accurate forecast. Table 2 shows the Skill score values for the 1- and 2-hour forecasts at each hour.

The positive S scores in Table 2 indicate the improvement of the OBS forecasts over the PCLIMO forecasts. The magnitudes of these values are also consistent with those found in VF and Hilliker and Fritsch (1999). In both the 1- and 2-hour forecasts, the S score has a tendency to decrease with decreasing cloud ceiling value. Incidentally, the number of occurrences of each cloud ceiling category decreases with decreasing height. The decrease in S and number of occurrences may be related. Also, the values for the 1-hour forecast of ceilings < 5000 ft at 02Z and 20Z are close to 0, indicating that persistence climatology is almost equal in performance at those times. Overall, however, the positive S values indicate that the OBS forecasts will produce a more accurate probability forecast of ceiling category occurrence.

Base on the results in Table 2 and at the request of SMG, Ms. Lambert will develop and test 3-hour forecast equations in the next quarter, and afterward begin writing the final report.

Table 2. Skill scores comparing the performance of the observations-based equations to that of the persistence climatology equations. A positive number indicates a percent improvement in forecast skill of the observations-based equations over the persistence climatology equations, and a negative number indicates a percent degradation.

Valid Time of Forecast	***1 Hour Forecast***			***2 Hour Forecast***		
	< 10 000 ft	**< 8000 ft**	**< 5000 ft**	**< 10 000 ft**	**< 8000 ft**	**< 5000 ft**
00Z	11.7	6.2	7.3	7.4	6.0	4.1
01Z	10.1	6.3	7.2	9.0	5.8	4.7
02Z	6.8	1.8	0.2	7.8	8.4	4.2
03Z	10.6	10.5	8.1	13.8	12.2	8.4
04Z	14.2	14.4	13.6	17.6	17.3	12.6
05Z	16.7	11.3	6.7	22.2	19.7	16.0
06Z	11.0	8.7	10.5	17.8	18.7	10.0
07Z	12.0	8.8	6.0	13.2	7.6	9.4
08Z	4.1	5.1	8.5	11.3	11.3	8.5
09Z	12.3	6.8	11.7	18.2	15.8	20.8
10Z	10.3	7.0	8.0	15.2	9.8	9.4
11Z	16.9	16.4	16.4	16.3	16.3	14.5
12Z	18.1	20.4	15.3	20.6	21.8	18.7
13Z	15.9	12.9	8.8	22.9	22.8	23.8
14Z	12.0	10.9	12.0	18.8	15.6	11.7
15Z	10.9	12.7	12.7	17.1	13.8	8.3
16Z	17.6	17.4	11.9	19.5	15.6	13.7
17Z	8.3	9.6	7.8	18.3	15.4	18.4
18Z	13.5	14.0	10.6	13.2	16.6	12.7
19Z	7.7	8.5	8.2	15.0	13.0	16.6
20Z	9.6	4.8	-0.6	7.8	6.8	13.0
21Z	11.2	7.9	3.2	16.1	9.5	3.5
22Z	13.2	10.4	9.7	11.5	9.9	12.7
23Z	15.0	13.4	9.5	19.4	16.1	13.3

References

Hilliker, J. L., and J. M. Fritsch, 1999: An observations-based statistical system for warm-season hourly probabilistic forecasts of low ceiling at the San Francisco International Airport. *J. Appl. Meteor.*, **38**, 1692-1705.

Vislocky, R. L., and J. M. Fritsch, 1997: An automated, observations-based system for short-term prediction of ceiling and visibility. *Wea. Forecasting*, **12**, 31-43.

2.2 TASK 004 INSTRUMENTATION AND MEASUREMENT

SUBTASK 12 SIGMET IRIS/OPEN PROCESSOR EVALUATION (DR. SHORT)

Phase II of the SIGMET IRIS/OPEN Processor Evaluation task calls for development of new radar products that will meet the operational requirements of the 45th Weather Squadron (45 WS) and SMG. The Interactive Radar Information System (IRIS) provides display and analysis of radar reflectivity data from the Weather Surveillance Radar, Model 74C (WSR-74C) located at Patrick Air Force Base (PAFB). Operational use of the radar and radar products includes evaluation of Launch Commit Criteria (LCCs) and FRs, and forecasting for ground operations.

In December, Dr. Short provided a status briefing to the 45 WS highlighting two main issues impeding progress on portions of the SIGMET/IRIS exploitation task. First, the SIGMET/IRIS software is proprietary and allows access to only a limited set of source code files for development of customized products. Access to most, if not all, source code files is necessary to develop the customized products defined in this task. The AMU task plan addressed this issue as a possible barrier to successful completion of the task. Second, production of the prototype products developed by the AMU is invoked by UNIX system commands that interact in a limited way with the SIGMET/IRIS Product Generator System. Application programming interfaces that are fully interactive, such as Graphical User Interface (GUI) tools, are not available to users in SIGMET/IRIS. In the present operational environment, the radar operator has full control of product configuration, product scheduling and product output through module-driven GUI tools. The Programmer's Manual lacks information on module interlacing that may be required to implement fully interactive generation of customized products in an operational environment.

Based on information provided in the status briefing, the 45 WS requested that the SIGMET/IRIS task be amended to discontinue AMU programming efforts for new radar products and develop seasonally-dependent radar scan strategies. In addition, the 45 WS requested AMU assistance in writing a request for quotation so that SIGMET can estimate the cost of building automated radar products.

Following the rescope of the task, Dr. Short began development of new scan strategies for the WSR-74C using a generalized method for determining the sequence of radar elevation angles that comprise a radar scan strategy. The method will be used to examine the utility of changing scan strategies in response to seasonal variations in the depth of convective activity and in the height of the electrically active region of clouds up to the -20ºC level. The annual climatology of sounding data from Cape Canaveral Air Force Station (CCAFS, 3-letter identifier - XMR) indicates that the height of the -20ºC isotherm is below 28 000 ft more than 98% of the time. The present WSR-74C scan strategy is designed for year-round use, such that the highest elevation angle intersects the 28 000 ft level over Space Launch Complex 17C, the nearest active launch complex to the radar. However, seasonal variations in the height of the -20ºC isotherm may allow the design of alternative scan strategies that provide better radar coverage as the seasons change. The method Dr. Short is developing will compare the vertical resolutions of alternative scan strategies. This will enable an evaluation of the impact of scan strategy changes on vertical resolution.

Figure 1 illustrates the generalized method with three elevation angles using simple geometry. It is known that the problem can be formulated as such, provided that the ground range is represented on a sphere with a radius 4/3 that of earth (Rinehart 1997). This accounts approximately for atmospheric refraction of the radar beam. The highest elevation angle is chosen based on a requirement to reach a given height at a given ground range in order to provide radar coverage up to that height over facilities at that range. The next elevation angle is chosen such that the vertical gap between the first and second elevation angles is a prescribed value at a fixed reference height. This vertical gap then determines all subsequent elevation angles. The problem involves choosing a vertical gap such that the lowest desired elevation angle is attained after N gaps, where the number of elevation angles in the scan strategy is N + 1. One possible procedure would be to make an initial guess for the vertical gap that is known to be too small and then to increase the guessed gap by a small increment, determining the resulting sequence of scan angles for each guess. The solution is found when the vertical gap forces the lowest elevation angle to be the desired value. The beam coverage factor can be set to any value. For the present scan strategy the beam coverage factor is set to one-half the radar beam width and the lowest elevation angle is 0.4º.

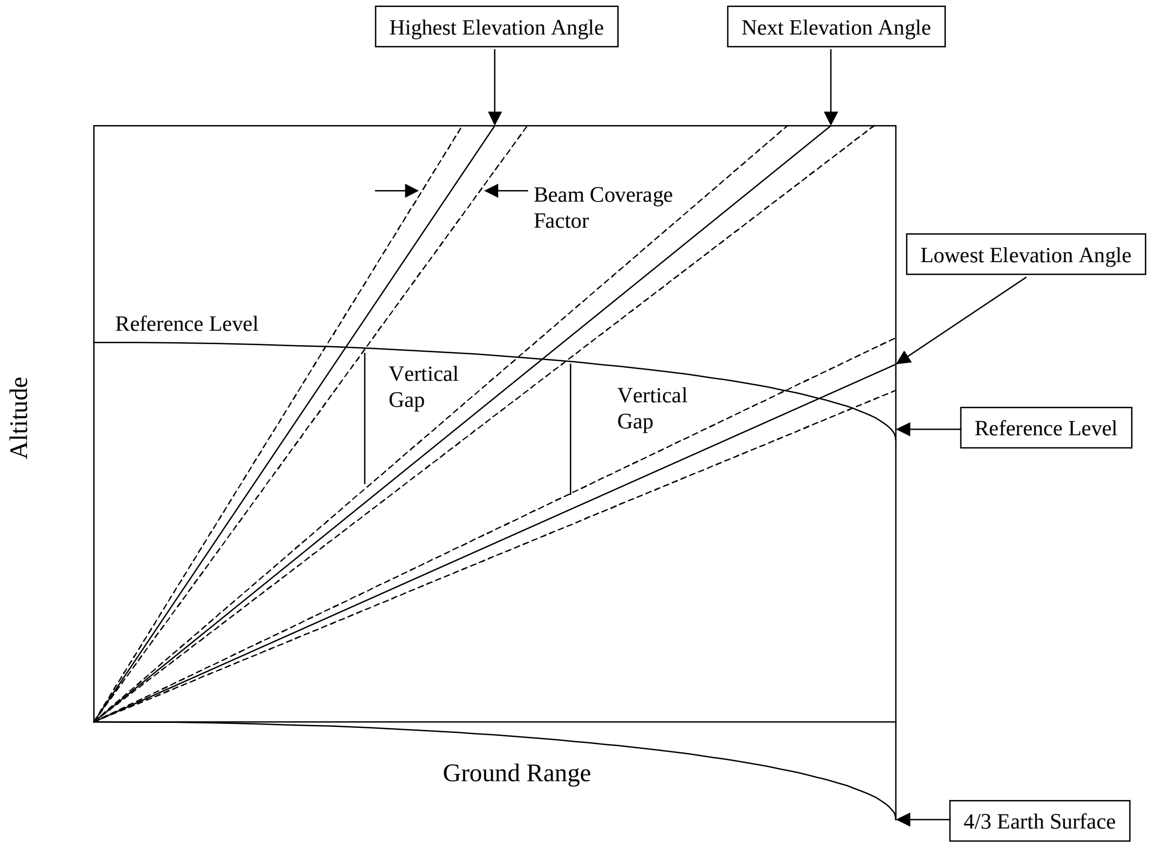

Figure 1. Schematic diagram of the methodology for determining the sequence of elevation angles for a radar scan, given the highest elevation angle, the lowest elevation angle and the number of elevation angles.

References

Rinehart, R. E., 1997: Radar for Meteorologists. *Rinehart Publications*, Grand Forks, 428 pp.

SUBTASK 12.1 AIRCRAFT POSITION RADAR OVERLAY (MR. WHEELER AND MR. DIANIC)

The aircraft position radar overlay task is funded by Kennedy Space Center (KSC) under AMU option hours. The AMU was tasked to superimpose the location of the research aircraft from the Airborne Field Mill (ABFM) experiment on WSR-74C SIGMET radar images. The ABFM experiment will collect data to allow safe revision of the lightning launch commit criteria to provide greater launch availability. During the June 2000 ABFM deployment, several problems were noted that will be addressed prior to the February 2001 campaign. These problems included drop-outs in the data transmission and issues with starting and stopping the data acquisition.

Preparations for the ABFM field experiment scheduled for February 2001 began in December 2000. Mr. Wheeler and Mr. Dianic discussed issues with the pre-processing software that decodes, filters, and reformats aircraft position data. Mr. Wheeler also talked with Mr. Oram of SMG about issues pertaining to updating the software that converts SIGMET/IRIS images to Man-computer Interactive Data Access System (McIDAS-X) files and overlays the aircraft position and altitude on the converted images in real time. The updated software that addresses these issues will be installed and tested in January 2001.

SUBTASK 13 MINI-SODAR EVALUATION (DR. SHORT AND MR. WHEELER)

The mini-SODAR is an acoustic wind profiler that provides a high spatial and temporal resolution vertical profile of wind speed and direction. The mini-SODAR in this evaluation provides wind profiles from 15 to 200 m with a gate spacing of 5 m at 1-minute intervals. Boeing plans to install a mini-SODAR at the new Space Launch Complex 37 (SLC-37) as a substitute for a tall wind tower. It will be used to evaluate the launch pad winds for the new Evolved Expendable Launch Vehicle (EELV) during ground operations and to evaluate LCCs during launch operations. In order to make critical GO/NO GO launch decisions, the 45 WS Launch Weather Officers (LWOs) and forecasters need to know the quality of mini-SODAR data. The AMU was tasked to perform an objective comparison between the SLC-37 mini-SODAR wind observations and those from the closest tall (≥ 204 ft) wind towers. However, Boeing has delayed the purchase of a mini-SODAR for the SLC-37 site. Therefore, the 45 WS requested that the AMU use data from the Range Standardization and Automation (RSA) mini-SODAR located at the False Cape site. This mini-SODAR is the same model to be purchased by Boeing and provides identical resolutions and range.

Mr. Wheeler began the mini-SODAR and wind tower data collection in October. Dr. Short and Mr. Wheeler began a comparative analysis of wind speed and direction observations from wind towers 313, 110, and 6 with data from the False Cape mini-SODAR. The December database of wind direction and speed data from the three towers was merged with the data from the mini-SODAR and imported into S-PLUS® for preliminary testing of the software and development of statistical analysis techniques.

2.3 TASK 005 MESOSCALE MODELING

SUBTASK 8 MESO-MODEL EVALUATION (MR. CASE)

The Eastern Range Dispersion Assessment System (ERDAS) is designed to provide emergency response guidance to the 45th Range Safety (45 SW/SE) in support of operations at the Eastern Range in the event of an accidental hazardous material release or an aborted vehicle launch. ERDAS uses the Regional Atmospheric Modeling System (RAMS) Numerical Weather Prediction (NWP) model to generate prognostic wind and temperature fields for input into ERDAS diffusion algorithms. The RAMS model is run twice per day and generates 24-hour forecasts initialized at 0000 and 1200 UTC. In addition to winds and temperatures, RAMS predicts a number of other meteorological quantities on four nested grids with horizontal resolutions of 60, 15, 5, and 1.25 km, respectively. Since the 1.25-km grid is centered over KSC/CCAFS, real-time RAMS forecasts provide an opportunity for improved weather forecasting in support of space operations through high-resolution NWP over the complex land-water interfaces of KSC/CCAFS. The 45 SW/SE and the 45 WS have tasked the AMU to evaluate the accuracy of RAMS for all seasons and under various weather regimes during 1999 and 2000.

Mr. Case completed most components of the objective and subjective evaluations of RAMS. For the objective evaluation, he compiled point error statistics for both the 1999-2000 cool (November to March) and 2000 warm seasons (May to September), and generated point error statistics under various meteorological regimes for the 2000 warm-season. For the subjective evaluation, Mr. Case completed the sea-breeze verification for the 1999 and 2000 warm-seasons. In addition, he compiled error statistics for a subjective precipitation and thunderstorm initiation verification. This quarterly report describes the methodology and presents results from the thunderstorm initiation verification that was conducted during the 2000 warm season.

Methodology for Thunderstorm Initiation Verification

A technique was developed to identify the first observed and forecast thunderstorm to the nearest hour on the RAMS innermost grid (grid 4). Following the methodology used to verify precipitation in the AMU ERDAS RAMS interim report (Case 2000), grid 4 was divided into 6 separate zones, 3 coastal and 3 inland (Figure 2a). Forecast and observed data were examined between the hours of 1500 and 2300 UTC daily from 1 May to 30 September 2000. This time window for validation was chosen for three reasons. First, warm-season thunderstorms occur most frequently in central Florida during these hours (Reap 1994). Second, both the 0000 and 1200 UTC RAMS forecast cycles from the same day overlap this time frame. Third, NWP models that are cold-started without a data assimilation scheme, such as the current operational RAMS, require a "spin-up" time period (~ few hours) before the model can adequately generate precipitation (Mohanty et al. 1996; Takano and Segami 1993). By starting the verification window at 1500 UTC, the 1200 UTC cycle of RAMS attains a 3-hour spin-up time for generating precipitation.

Archived Cloud to Ground Lightning Surveillance System (CGLSS) data and Geostationary Operational Environmental Satellite-8 (GOES-8) visible imagery were used to identify the first observed thunderstorm in each zone of RAMS grid 4 on an hourly basis. Since NWP models such as RAMS do not explicitly predict lightning and thunderstorms, an empirical technique was adopted to define formally a model-predicted thunderstorm. Using results from an east-central Florida dual-Doppler observational study conducted during the Convection and Precipitation/Electrification Experiment (CaPE, Yuter and Houze 1995a; Yuter and Houze 1995b), a model thunderstorm was defined by a predicted vertical velocity of 2 m s^{-1} or greater at 7 km height in conjunction with a precipitation rate of at least 5 mm h^{-1} (0.2 in. h^{-1}). This definition ensures that the model convection and updraft has reached a height where mixed-phase water particles co-exist, a condition found in electrified clouds (Bringi et al. 1997).

For each day that RAMS correctly predicted the occurrence of a thunderstorm within the grid-4 domain, the spatial and timing accuracy of the thunderstorm initiation were evaluated. For the spatial accuracy, the number of days were counted in which RAMS correctly predicted the location of thunderstorm initiation in one or more zones, irrespective of timing. For the timing accuracy, the number of days were counted in which RAMS correctly predicted the initiation time exactly (0-hour difference between observations and forecast), within 1 hour (-1 to +1 hour error), within 2 hours (-2 to +2 hour error), and within 3 hours (-3 to +3 hour error) of the observed time, irrespective of spatial accuracy.

Thunderstorm Initiation Verification Results

Following the definitions given above, the first observed and RAMS-predicted thunderstorm in the 1500–2300 UTC time frame (if any) were identified in each of the six zones for both the 0000 and 1200 UTC RAMS forecast cycles. An example from 14 May 2000 shows one of the thunderstorm days in which RAMS performed very well in predicting the first and subsequent thunderstorms (Figure 2). The GOES-8 visible imagery overlaid with CGLSS lightning strikes shows the first thunderstorm in zone 6 at 1800 UTC (Figure 2b). Additional small thunderstorms occur in portions of zones 2, 3, 5, and 6 over the next hour (Figure 2c). The RAMS 6-hour forecast from the 1200 UTC cycle (valid 1800 UTC) depicts the first thunderstorm in zone 6 during the same hour as observed (Figure 2e). RAMS also accurately predicts the locations of the thunderstorms during the next hour as shown in Figure 2f. This example is certainly the exception rather than the rule during the 2000 Florida warm season, since on most days the timing and spatial errors were significant. However, this case illustrates that accurate convective-scale forecasts are possible over east-central Florida when running a NWP model such as RAMS at sufficiently high resolutions.

The results of the thunderstorm initiation verification are summarized in three ways, in order of increasing stringency. First, the ability of RAMS to predict correctly the occurrence of thunderstorms anywhere on grid 4 for a given day is summarized in Tables 4 and 5. Second, the ability of RAMS to predict correctly the occurrence of thunderstorms in each of the 6 zones is shown in Figure 3. Finally, the specific timing and zone verification of thunderstorm initiation is given in Table 5.

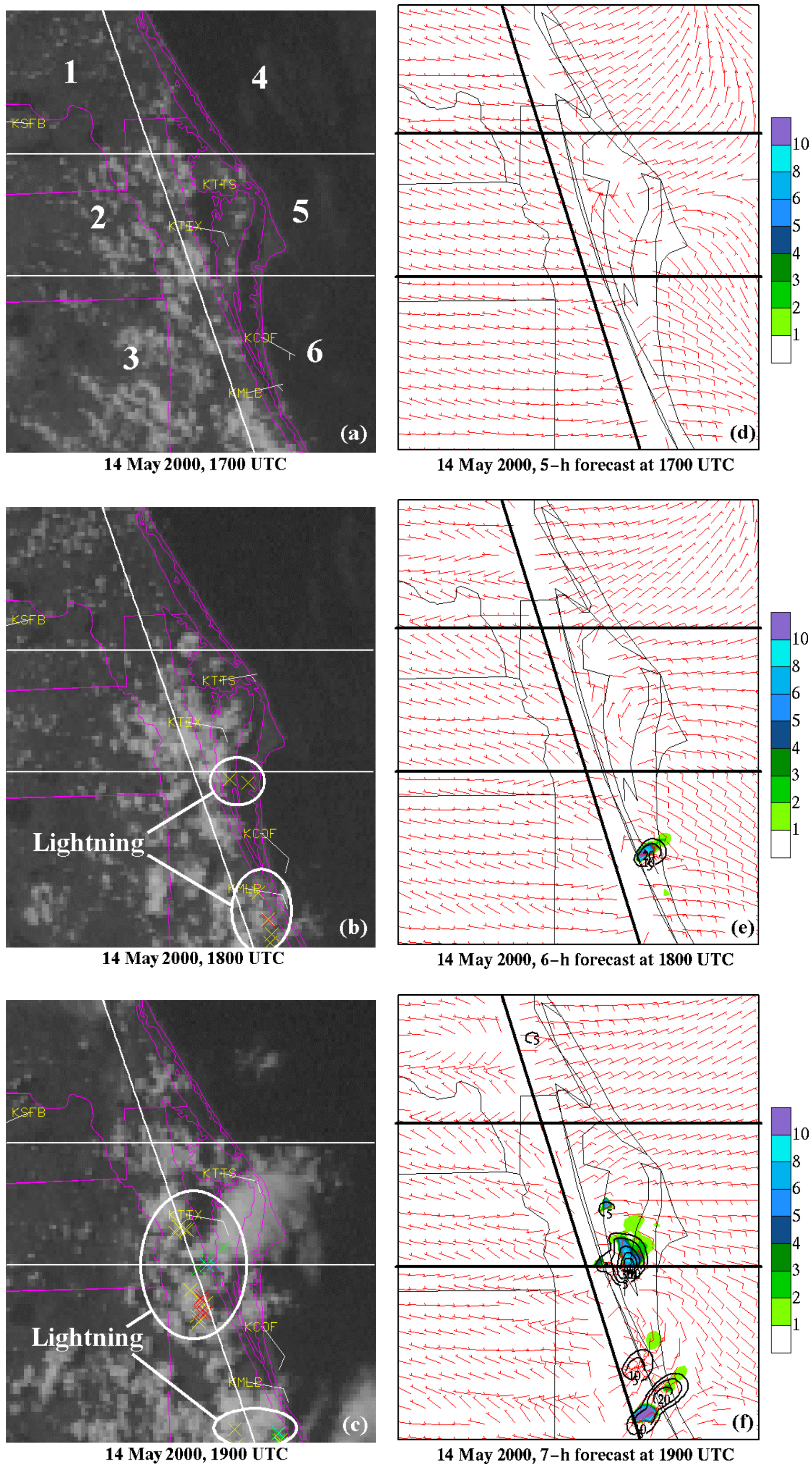

Figure 2. Hourly GOES-8 visible satellite imagery and surface winds overlaid with CGLSS cloud-to-ground lightning strikes (a, b, and c, denoted by a colored 'X') compared to RAMS forecast surface winds, 7-km vertical velocity (m s^{-1}), and surface precipitation rate (mm h^{-1}) (d, e, and f) on 14 May 2000 over the area of RAMS grid 4. Valid times for the observed plots are a) 1700 UTC, b) 1800 UTC, and c) 1900 UTC and the corresponding RAMS forecast plots at d) 1700 UTC, e) 1800 UTC, and f) 1900 UTC.

According to Tables 4 and 5, the 1200 UTC RAMS forecast cycle predicted the occurrence of a thunderstorm day on grid 4 much better than the 0000 UTC cycle. In the 1200 UTC cycle, the number of correctly predicted thunderstorm days is higher than the 0000 UTC cycle in combination with fewer missed forecasts (Table 3). As a result, the 1200 UTC cycle has a higher probability of detection (POD) than the 0000 UTC cycle (Table 4). However, the 1200 UTC cycle does have a slightly greater tendency towards false alarms and over-predicting thunderstorm days, as indicated by the slightly higher false alarm rate (FAR) and a bias greater than 1.0 (Table 4). In this convention, a bias value greater than 1.0 indicates over-predicting a quantity whereas a bias less than 1.0 is under-prediction.

Table 3. A contingency table of the occurrence of RAMS predicted versus observed thunderstorms for a given day, verified on grid 4 during the 2000 Florida warm season.

0000 UTC Forecast Cycle	**Observed T-storms**	**No Observed T-storms**
Forecast T-storms	36	11
No Forecast T-storms	36	46
1200 UTC Forecast Cycle	**Observed T-storms**	**No Observed T-storms**
Forecast T-storms	72	25
No Forecast T-storms	11	38

Table 4. Categorical and skill scores of RAMS forecast versus observed thunderstorms on a given day, associated with the contingencies in Table 3.

Parameter	**0000 UTC Forecast Cycle**	**1200 UTC Forecast Cycle**
Probability of Detection	0.50	0.87
False Alarm Rate	0.23	0.26
Bias	0.65	1.17

Figure 3 shows the POD and FAR for the 0000 and 1200 UTC RAMS cycles as a function of zone in grid 4. These results again show that the 1200 UTC cycle better predicts the occurrence of thunderstorms for all zones, based on the significantly higher PODs (Figure 3a). The FARs are similar except for the northwest and southeast zones (1 and 6). The 0000 UTC cycle had a higher FAR in zone 6 whereas the 1200 UTC cycle had a larger FAR in zone 1 (Figure 3b). It is interesting to note that in both forecast cycles, RAMS has the lowest POD for thunderstorm occurrence in zone 6.

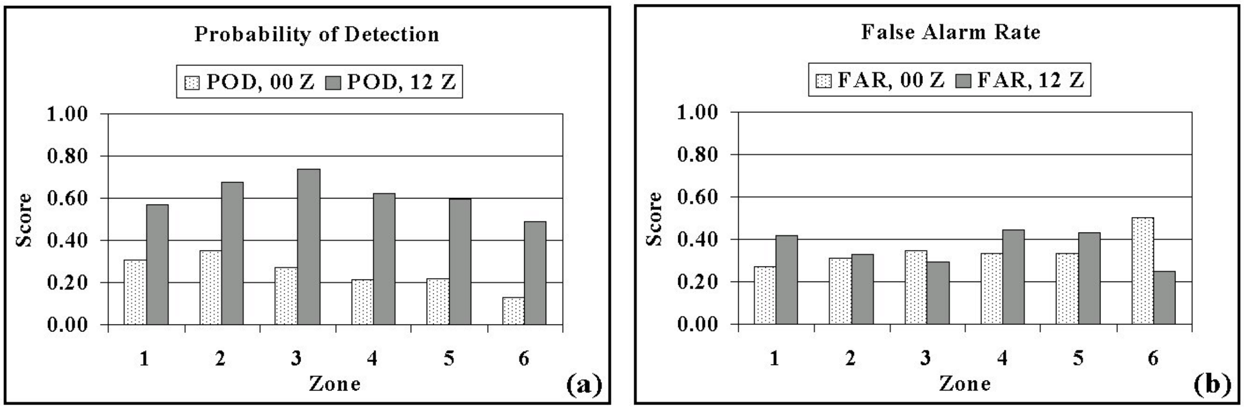

Figure 3. Categorical scores are shown for the verification of the 0000 and 1200 UTC RAMS forecast cycles in predicting the occurrence of a thunderstorm on a given day during the 2000 Florida warm season. The scores shown in this figure are a) probability of detection and b) false alarm rate.

Table 5 summarizes the spatial and timing results of the RAMS forecast thunderstorm initiation for the 0000 and 1200 UTC cycles. In general, both forecast cycles are comparable in terms of the spatial accuracy, whereas the 1200 UTC cycle exhibits slightly more favorable results in the timing of thunderstorm initiation. Spatially, both forecast cycles correctly predicted thunderstorm initiation in one or more zones about half the time (58% in 0000 UTC cycle and 49% in 1200 UTC cycle, Table 5). The slightly poorer performance in the 1200 UTC cycle could be attributed to the larger sample size of correct forecast thunderstorm days. In the timing accuracy, only 8 % (17%) of the correctly predicted thunderstorm days experienced an exact initiation time to the nearest hour for the 0000 UTC (1200 UTC) cycle. Meanwhile, RAMS correctly predicted the thunderstorm initiation time to within 3 hours of the observed time about 75% of all days for both forecast cycles (slightly higher in the 1200 UTC forecasts).

These results suggest that the more recent 1200 UTC initialization of RAMS to the time of convection initiation improves the predictions of the occurrence of thunderstorms, but does not considerably improve the accuracy of the predicted location and timing of thunderstorm initiation. This somewhat limited skill in predicting the location and timing of thunderstorm initiation (and convective precipitation forecasts in general) could be caused by three characteristics of the current RAMS configuration. First, the lateral boundaries of grid 4, particular the eastern boundary, are not significantly displaced from the area of interest (e.g. the Florida east coast). Expansion of grid 4 could help to alleviate the negative impacts and errors that can be caused by lateral boundary interactions with the coarser grid (Warner et al. 1997). Second, errors in precipitation and the vertical distribution of latent heating, associated with the parameterized treatment of convection on the outer grids, greatly impact the explicit convective forecasts on the inner grid (Warner and Hsu 2000). In fact, Warner and Hsu (2000) found that different precipitation parameterizations on the outer grids produced up to a factor of 3 difference in the 24-hour precipitation forecasts. Finally, a more sophisticated and frequent mesoscale initialization and data assimilation scheme is needed for RAMS, where high-resolution, continuous observational data such as Weather Surveillance Radar-1988 Doppler (WSR-88D) and GOES-8 satellite data are assimilated and brought into balance with the model equations.

Table 5. A list of the number of days (and percent correct) that RAMS correctly identified on one or more of the grid-4 zones for thunderstorm initiation, and the number of days (and percent correct) that RAMS predicted thunderstorm initiation to the nearest hour (correct), within 1 hour (± 1 hour), within 2 hours (± 2 hours), and within 3 hours (± 3 hours). The total number of days are taken from the correct prediction of a thunderstorm day, given in the upper-left contingency panels in Table 3.

	0000 UTC Cycle			***1200 UTC Cycle***		
Parameter	**Number**	**Total**	**% Correct**	**Number**	**Total**	**% Correct**
≥ 1 zone correct	21	36	58	35	72	49
Correct timing	3	36	8	12	72	17
Timing within 1 h	13	36	36	30	72	42
Timing within 2 h	19	36	53	45	72	63
Timing within 3 h	26	36	72	57	72	79

For more information, or to obtain a copy of the interim report, contact Mr. Jonathan Case by phone at 321-853-8264 or by email at case.jonathan@ensco.com.

References

Bringi, V. N., K. Knupp, A. Detwiler, L. Liu, I. J. Caylor, and R. A. Black, 1997: Evolution of a Florida thunderstorm during the Convection and Precipitation/Electrification Experiment: The case of 9 August 1991. *Mon. Wea. Rev.*, **125**, 2131-2160.

Case, J., 2000: Interim report on the evaluation of the Regional Atmospheric Modeling System in the Eastern Range Dispersion Assessment System. NASA Contractor Report CR-2000-208576, Kennedy Space Center, FL, 102 pp. [Available from ENSCO, Inc., 1980 N. Atlantic Ave., Suite 230, Cocoa Beach, FL 32931].

Mohanty, U. C., A. Kasahara, and R. Errico, 1986: The impact of diabatic heating on the initialization of a global forecast model. *J. Meteor. Soc. Japan*, **64**, 805-817.

Reap, R. M., 1994: Analysis and prediction of lightning strike distributions associated with synoptic map types over Florida. *Mon. Wea. Rev.*, **122**, 1698-1715.

Takano, I. and A. Segami, 1993: Assimilation and initialization of a mesoscale model for improved spin-up of precipitation. *J. Meteor. Soc. Japan*, **71**, 377-391.

Warner, T. T., R. A. Peterson, and R. E. Treadon, 1997: A tutorial on lateral boundary conditions as a basic and potentially serious limitation to regional numerical weather prediction. *Bull. Amer. Meteor. Soc.*, **78**, 2599-2617.

____, and H-M. Hsu, 2000: Nested-model simulation of moist convection: The impact of coarse-grid parameterized convection on fine-grid resolved convection. *Mon. Wea. Rev.*, **128**, 2211-2231.

Yuter, S. E., and R. A. Houze Jr., 1995a: Three-dimensional kinematic and microphysical evolution of Florida cumulonimbus. Part I: Spatial distribution of updrafts, downdrafts, and precipitation. *Mon. Wea. Rev.*, **123**, 1921-1940.

____, and ____, 1995b: Three-dimensional kinematic and microphysical evolution of Florida cumulonimbus. Part II: Frequency distributions of vertical velocity, reflectivity, and differential reflectivity. *Mon. Wea. Rev.*, **123**, 1941-1963.

SUBTASK 10 LOCAL DATA INTEGRATION SYSTEM PHASE III (MR. CASE)

The Local Data Integration System (LDIS) task emerged out of the need to simplify the generation of short-term weather forecasts in support of launch, landing, and ground operations. The complexity of creating short-term forecasts has increased due to the variety and disparate characteristics of available weather observations. Therefore, the goal of the LDIS task is to generate high-resolution weather analysis products that may enhance the operational forecasters' understanding of the current state of the atmosphere, resulting in improved short-term forecasts. In Phase I, the AMU configured a prototype LDIS using the Advanced Regional Prediction System (ARPS) Data Analysis System (ADAS). The LDIS integrated all available weather observations into gridded analyses covering east-central Florida. In Phase II, the AMU simulated a real-time LDIS configuration using two weeks of archived data. The LDIS Phase III task calls for AMU assistance to the SMG and the National Weather Service in Melbourne (NWS MLB) to install a working real-time LDIS that routinely generates high-resolution products for operational guidance.

SMG Installation

During this past quarter, the AMU provided remote assistance to SMG to correct a problem in the cloud analysis portion of the ADAS. The real-time cloud analysis products were not being generated properly during times when no surface observations of clouds were available. Mr. Case corrected the portion of the ADAS code causing the problem and sent the updated file to SMG with instructions on how to rebuild the ADAS program. Mr. Oram of SMG implemented these changes and the cloud analysis products are now generated at each 15-minute LDIS analysis time.

NWS MLB Installation

The AMU assistance to the NWS MLB focused on two specific areas: data availability and the WSR-88D data ingest procedure. The data availability problem at the NWS MLB office involves obtaining the national data sets and local KSC/CCAFS wind-tower and profiler observations in a ready-to-use format required for ingest into LDIS. The AMU and the NWS MLB have pursued various avenues to obtain these data in the proper format, but with little success. Thus, the AMU, NWS MLB, and SMG collaborated on a technique that allows the NWS MLB to use post-processed data from the data ingestors at SMG for their LDIS. With the help of NWS Southern Region Headquarters (SRH), the NWS MLB now obtains the post-processed data sets required for LDIS. SMG posts the processed data sets every 15 minutes onto the SRH file transfer protocol (ftp) server. The NWS MLB subsequently downloads these data from the SRH ftp server for use in LDIS.

The other significant issue is the ingest procedure for real-time level II WSR-88D data. In order to access and map the real-time level II WSR-88D reflectivity and radial velocity data onto the ADAS analysis grid, two utilities from the National Severe Storms Laboratory (NSSL) are required: the Radar Interface and Data Distribution System (RIDDS) software, and the A2IO utility. Since NSSL maintains and supports these software utilities only for a Sun/Solaris hardware platform, the AMU downloaded and built both these software packages on a Hewlett Packard (HP) workstation, the LDIS platform used at both SMG and the NWS MLB. The RIDDS software is the primary link between the real-time level II data and the LDIS workstation. Unfortunately, the current configuration of the RIDDS software does not properly process the level II data for ingest into the LDIS. Further diagnosis and/or assistance from NSSL is needed to determine the cause of the problem. Therefore, the NWS MLB is currently running LDIS with the same real-time observations as SMG except for WSR-88D data.

SUBTASK 11 EXTENSION / ENHANCEMENT OF THE ERDAS RAMS EVALUATION (MR. CASE AND MR. DIANIC)

The Extension / Enhancement of the ERDAS RAMS Evaluation is being funded by KSC under AMU option hours. During the course of the evaluation under Subtask 8 (Meso-Model Evaluation), the AMU discovered a systematic low-level cold bias in the RAMS forecasts. In addition, several RAMS forecasts were not successfully run in real-time due to various technical issues. As a result, KSC tasked the AMU to re-run historical RAMS forecasts to improve the archived data base, and to perform sensitivity tests to identify the possible cause(s) for the model cold bias. Also, depending on the remaining funds in the options hours task, the AMU will explore the possibility of transferring real-time RAMS forecasts to the NWS MLB and SMG offices, and to improve the ENSCO-generated graphical user interface that verifies RAMS forecasts in real time.

AMU work in this quarter focused on four areas in the extension task: installation of ERDAS RAMS and associated utilities at the AMU, data recovery, sensitivity experiments, and the data transfer mechanism. Mr. Dianic installed and tested ERDAS RAMS on an AMU workstation, as well as an interface to convert and view RAMS forecast data using the Visualization in 5 Dimensions (Vis5D) software. The Vis5D software provides a platform to easily view and diagnose gridded forecast data in a short amount of time. He began recovering RAMS 3-grid forecast runs during the 1999-2000 cool season that were lost due to a disk crash. Mr. Dianic also completed the 4-grid RAMS sensitivity forecasts using Eta 0-hour rather than 12-hour forecasts as background fields for the model initial condition. He ran a sensitivity experiment using the Mahrer and Pielke (1977) radiation scheme rather than the current operational Chen and Cotton (1988) scheme. Finally, he continued to develop and test a possible real-time data transfer mechanism that will be able to send RAMS forecast output to the SMG and NWS MLB offices.

RAMS Sensitivity Experiment Using Eta 0-hour Forecasts

Methodology

This sensitivity test involved running 24-hour forecasts of the full 4-grid configuration of RAMS using the most recent Eta 0-hour rather than 12-hour forecasts as a background fields for the RAMS initial condition. In addition, 0–24 hour forecasts from the most recent Eta model were used as boundary conditions rather than the 12–36 hour Eta forecasts. This experiment was run to determine if using more recent Eta forecasts would have any impact on the subsequent RAMS point forecast errors. The experiment was conducted from late March to the end of September 2000 in order to obtain a sufficiently large sample size for both the 0000 and 1200 UTC forecast cycles. The point error statistics from these experimental model runs were compiled and compared to the original RAMS forecasts using Eta 12-hour forecasts as background fields (and 12–36 hour Eta forecasts as boundary conditions).

Results

In general, very little change in the surface point error statistics occurred when using more recent Eta model output in the RAMS initial condition. Figures 4 and 5 show the 1200 UTC RAMS cycle point error statistics for the KSC/CCAFS wind-tower network, computed at 1.8 m (6 ft) for temperature and 16.5 m (54 ft) for wind direction. Both the operational (4-oper) and experimental (4-exp.) RAMS forecasts have root mean square (RMS) errors between 1.5 and 4.0°C during the course of the 24-hour forecast (Figure 4b). In addition, the biases are nearly identical in magnitude for all forecast hours, with both RAMS forecasts demonstrating a daytime cold bias near -2°C between forecast hours 3 and 12 (Figure 4c). The most variation between 4-oper and 4-exp. occurs in the error standard deviation, where a 0.5–1.0°C difference is observed between forecast hours 6 and 18.

In addition to negligible changes in surface temperature errors, only minor differences occurred in wind-direction errors as well. The wind-direction RMS errors of 4-oper and 4-exp. are generally within 5–10° of each other during all 24 forecast hours (Figure 5a). The most significant difference occurs in the wind-direction bias, where the 4-exp. forecasts have a more negative bias compared to 4-oper, especially between forecast hours 3 and 9 (Figure 5b). However, the magnitude of these bias differences is inconsequential compared to the overall model errors, given by the RMS error. The AMU has not yet analyzed the results of this sensitivity test at upper-levels of the atmosphere.

Based on the surface point error results at the KSC/CCAFS wind-tower network, it appears as though the more recent Eta background field and boundary conditions does not substantially change or improve the RAMS point error statistics on the innermost grid 4. This small change in errors may be a result of the time frame used in this study. Most of the forecasts for this study were run during the 2000 Florida warm season (May–September) and large-scale meteorological regimes may not have played a substantial role in governing the RAMS errors. Nonetheless, the results of this sensitivity experiment are important because the surface errors demonstrate that using a more up-to-date background field does not significantly improve the surface model errors on RAMS grid 4.

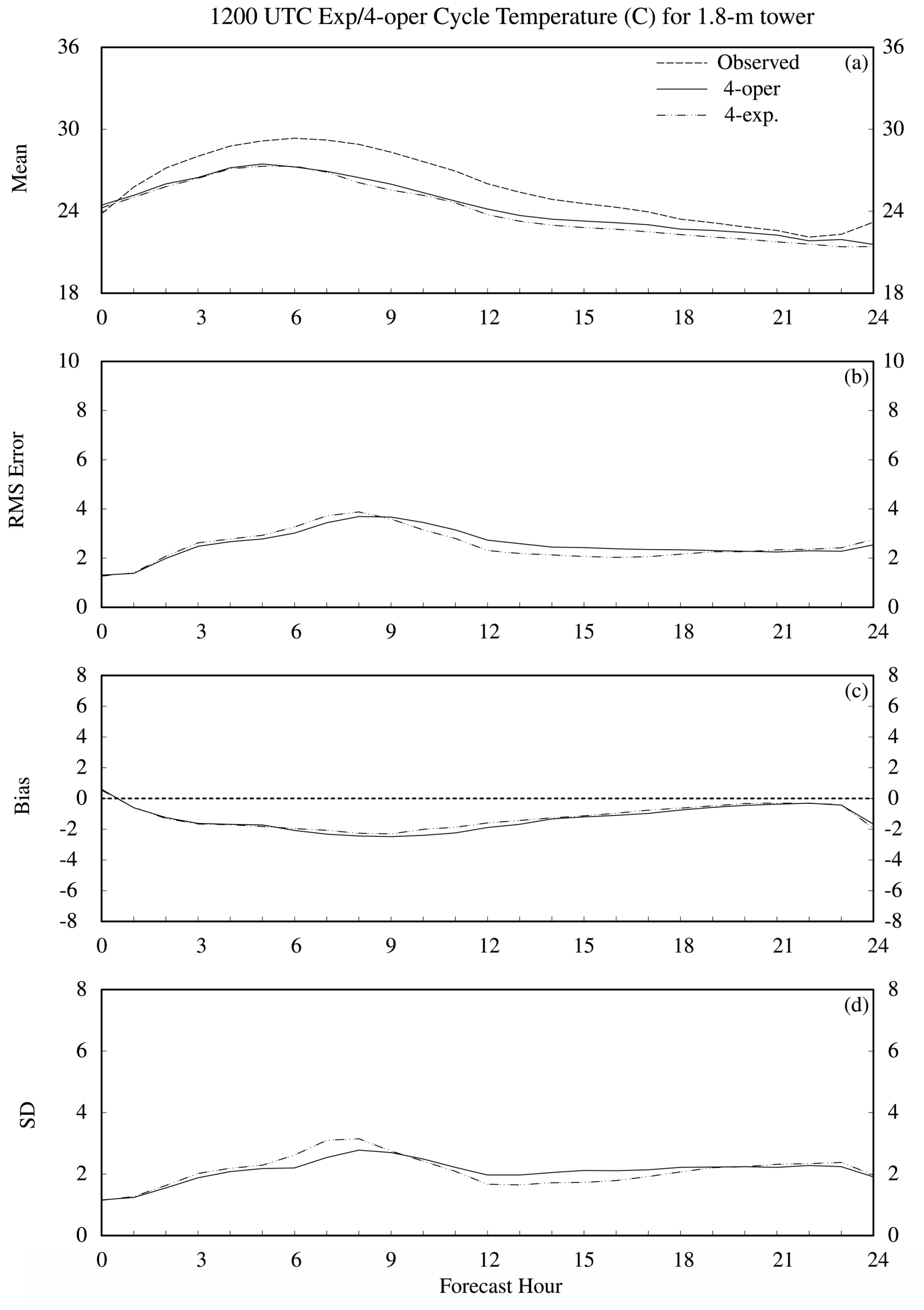

Figure 4. A graphical trace that displays a comparison between the 1200 UTC forecast cycle surface temperature errors (°C) from the operational RAMS and the RAMS experiment using Eta 0-hour forecasts for background fields. Surface temperatures are verified at the 1.8 m level of the KSC/CCAFS wind tower network. Parameters plotted as a function of forecast hour for both the operational (4-oper) and experimental RAMS (4-exp.) include: a) mean observed temperature, mean operational 4-grid forecast temperature, and mean experimental 4-grid forecast temperature, b) RMS error, c) bias, and d) error standard deviation. The plotting convention is a solid line for the 4-oper forecasts, dot-dashed line for the 4-exp. forecasts, and a dashed line for observed values.

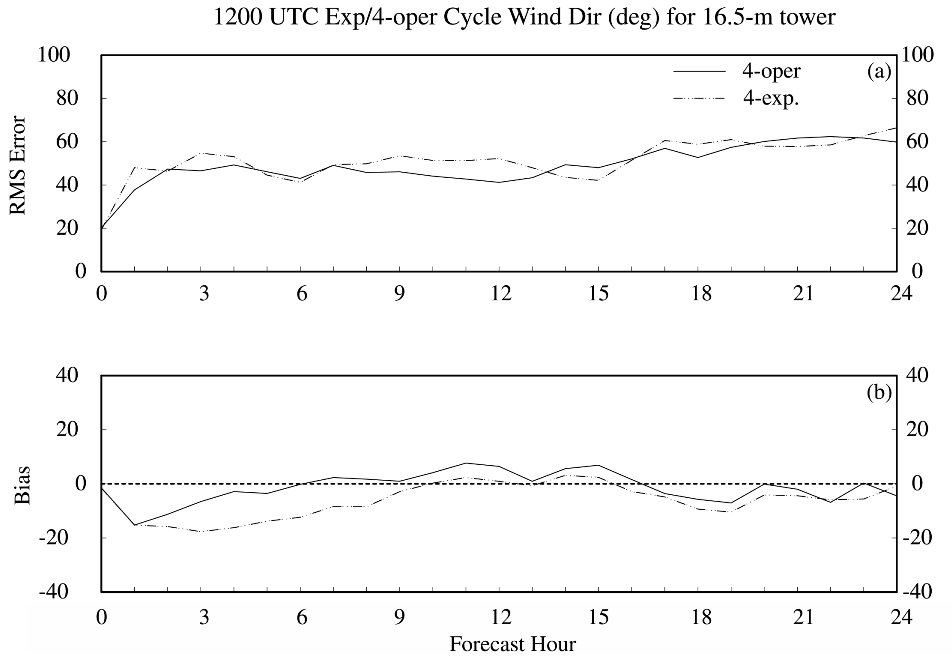

Figure 5. A graphical trace that displays a comparison between the 1200 UTC forecast cycle near-surface wind direction errors (degrees) from the operational RAMS and the RAMS experiment using Eta 0-hour forecasts for background fields. Near-surface wind direction is verified at the 16.5-m level of the KSC/CCAFS wind tower network. Parameters plotted as a function of forecast hour for both the operational (4-oper) and experimental RAMS (4-exp.) include: a) RMS error and b) bias. The plotting convention is a solid line for the 4-oper errors and a dot-dashed line for the 4-exp. errors.

References

Chen, S., and W. R. Cotton, 1988: The sensitivity of a simulated extratropical mesoscale convective system to longwave radiation and ice-phase microphysics. *J. Atmos. Sci.*, **45**, 3897-3910.

Mahrer, Y., and R. A. Pielke, 1977: A numerical study of the airflow over irregular terrain. *Beitr. Phys. Atmos.*, **50**, 98-113.

2.4 AMU CHIEF'S TECHNICAL ACTIVITIES (DR. MERCERET)

Dr. Merceret participated in a planning meeting with the University of Central Florida to develop a research approach for the use of WSR-88D and the Texas Florida Underflight Experiment - B (TEFLUN-B) rain gauge, disdrometer, and wind profiler data. The approach will use the data to validate or improve theoretical analyses of the effect of vertical wind velocity on Z-R relationships, the effect of horizontal advection on radar measurement of rainfall, and the effect of falling precipitation on wind profiler measurements. He also began detailed preparations for the ABFM field campaign scheduled for February 2001. The experiment will collect data to allow safe revision of the lightning launch commit criteria to provide greater launch availability.

2.5 TASK 001 AMU OPERATIONS

Mr. Wheeler attended the annual Man-computer Interactive Data Access System (McIDAS) Users Group (MUG) Meeting at the Space Science and Engineering Center in Madison, WI. Since McIDAS-X is still the operational weather display system for the 45 WS and SMG, AMU attendance at the MUG meetings is important to maintain AMU proficiency on the system and keep apprised of planned improvements and upgrades that will affect users. He also installed and tested the AMU's new tape backup unit to make sure the device and software would backup and restore files to both the desktop and UNIX workstations. This backup unit will upgrade and replace the current IBM tape library system.

Dr. Manobianco attended the National Weather Association Annual Meeting in Gaithersburg, MD. He gave an oral presentation describing the cool season ERDAS RAMS evaluation and was invited to serve as a panelist for the conference-wide forum on mesoscale numerical weather prediction. He also visited SMG at Johnson Space Center (JSC) from 27 November to 1 December to observe weather operations in support of the Shuttle Transportation System (STS) 97 launch. While at JSC, Dr. Manobianco discussed issues with the LDIS running in real time at SMG and plans for the LDIS follow-on task where the AMU will assist SMG with the configuration and installation of the ARPS. Overall, the visit helped maintain the two-way flow of information between SMG and the AMU by face-to-face discussions of work that is usually described only through written reports.

NOTICE

List of Acronyms

30 SW	30th Space Wing
30 WS	30th Weather Squadron
45 LG	45th Logistics Group
45 OG	45th Operations Group
45 SE	45th Range Safety
45 SW	45th Space Wing
45 WS	45th Weather Squadron
ABFM	Airborne Field Mill
ADAS	ARPS Data Analysis System
AFRL	Air Force Research Laboratory
AFSPC	Air Force Space Command
AFWA	Air Force Weather Agency
AMU	Applied Meteorology Unit
ARPS	Advanced Regional Prediction System
B	Brier Score
CCAFS	Cape Canaveral Air Force Station
CGLSS	Cloud to Ground Lightning Surveillance System
CSR	Computer Sciences Raytheon
EELV	Evolved Expendable Launch Vehicle
EOM	End of Mission
ERDAS	Eastern Range Dispersion Assessment System
FAR	False Alarm Rate
FR	Shuttle Flight Rules
FSL	Forecast Systems Laboratory
FSU	Florida State University
FY	Fiscal Year
GOES	Geostationary Operational Environmental Satellite
HP	Hewlett Packard
IRIS	SIGMET's Integrated Radar Information System
JSC	Johnson Space Center
KSC	Kennedy Space Center
LCC	Launch Commit Criteria
LDIS	Local Data Integration System
McIDAS	Man-computer Interactive Data Access System
MLB	Melbourne, FL 3-Letter Identifier
MSFC	Marshall Space Flight Center
MUG	McIDAS Users Group
NASA	National Aeronautics and Space Administration
NCAR	National Center for Atmospheric Research
NOAA	National Oceanic and Atmospheric Administration
NSSL	National Severe Storms Laboratory

List of Acronyms

NWP	Numerical Weather Prediction
NWS MLB	National Weather Service in Melbourne, FL
OBS	Observations-Based equations
PAFB	Patrick Air Force Base
PCLIMO	Persistence Climatology equations
POD	Probability of Detection
RAMS	Regional Atmospheric Modeling System
RIDDS	Radar Interface and Data Distribution System
RMS	Root Mean Square
RSA	Range Standardization and Automation
RTLS	Return to Launch Site
S	Skill Score
SLF	Shuttle Landing Facility
SMC	Space and Missile Center
SMG	Spaceflight Meteorology Group
SRH	NWS Southern Region Headquarters
STS	Shuttle Transportation System
TEFLUN-B	Texas Florida Underflight Experiment - B
TTS	SLF 3-Letter Identifier
USAF	United States Air Force
UTC	Universal Coordinated Time
VF	Vislocky and Fritsch, 1997
WSR-74C	Weather Surveillance Radar, model 74C
WSR-88D	Weather Surveillance Radar 1988 Doppler
WWW	World Wide Web
XMR	CCAFS 3-Letter Identifier

Appendix A

AMU Project Schedule 31 January 2001				
AMU Projects	Milestones	Scheduled Begin Date	Scheduled End Date	Notes/Status
Statistical Forecast Guidance (Ceilings)	Determine Predictand(s)	Aug 98	Sep 98	Completed
	Data Collection, Formulation and Method Selection	Sep 98	Apr 99	Completed
	Equation Development, Tests with Independent Data, and Tests with Individual Cases	Apr 00	Dec 00	Completed
	Prepare Products, Final Report for Distribution	Jan 00	Feb 01	On Schedule
Statistical Forecast Guidance (Winds)	Determine Predictand(s)	Feb 01	Mar 01	On Schedule
	Data Reduction, Formulation and Method Selection	Mar 01	May 01	On Schedule
	Equation Development, Tests with Independent Data, and Tests with Individual Cases	May 01	Sep 01	On Schedule
	Prepare Products, Final Report for Distribution	Sep 01	Dec 01	On Schedule
Meso-Model Evaluation	Develop ERDAS/RAMS Evaluation Protocol	Feb 99	Mar 99	Completed
	Perform ERDAS/RAMS Evaluation	Apr 99	Sep 99	Completed
	Extend ERDAS/RAMS Evaluation	Oct 99	Nov 00	Completed
	Interim ERDAS/RAMS Report	Dec 99	Aug 00	Completed
	Final ERDAS/RAMS Report	Oct 00	Jan 01	Behind Schedule - Need to perform additional sea-breeze verifications
SIGMET IRIS Processor Evaluation Phase II	Develop and transition new products to 45 WS IRIS station	Apr 00	Apr 01	Rescheduled – Customer to re-scope task based on AMU preliminary results
	Final Report	May 01	Jun 01	On Schedule

AMU Project Schedule

31 January 2001

AMU Projects	Milestones	Scheduled Begin Date	Scheduled End Date	Notes/Status
LDIS Extension: Phase III	Assistance in installation at NWS MLB	Jan 00	Jan 01	Completed – Except for radar data ingestor
	Assistance in installation at SMG	Apr 00	Jul 00	Completed
	Memorandum describing LDIS transition to real-time operations	Jul 00	Jan 01	Draft completed – Will be distributed in Jan 01
	Technical collaboration with SMG towards a conference paper	Aug 00	Jan 01	Collaboration on abstract to occur in Jan 01
ERDAS RAMS Extension Task	Memorandum summarizing data transfer feasibility to SMG & NWS MLB	Jul 00	Jan 01	Behind Schedule – Debugging remote connection
	Enhancement of verification Graphical User Interface	Apr 00	Feb 01	On Schedule
	Implement data transfer	Sep 00	Jan 01	Behind Schedule– Debugging remote connection
	Input of methodology and results into ERDAS RAMS final report	Nov 00	Jan 01	Behind Schedule – Waiting to finish all sensitivity tests
Mini-SODAR Evaluation	Collection and Processing of data	Oct 00	Sep 01	On Schedule
	Analysis and objective comparison	Jan 01	Oct 01	On Schedule
	Final Report	Oct 01	Apr 02	On Schedule